EDELWEISS PUBLICATIONS
OPEN ACCESS

Volume 1 • Issue 1 | Page 1 of 5

Nanomaterial Chemistry and Technology

Research Article

Synthesis and Electrocatalytic Properties of Materials Based On Graphene Structures

MO Danilov[1], IA Rusetskii[1]*, IA Slobodyanyuk[1], IA Farbun[2] and G Ya Kolbasov[1]

Abstract

Catalysts for oxygen electrodes based on graphene structures have been obtained by the chemical synthesis. Oxidizing and reducing agents were selected on the basis of their standard redox potentials. For the obtained materials, the morphology, physical and chemical properties, and electrocatalytic activity for the reaction of oxygen reduction have been investigated. It was shown that the synthesized graphene oxide and reduced graphene oxide are promising catalyst carriers for the oxygen electrode of fuel cells, which can replace commercial electrode materials containing platinum. The specific capacity of the electrode based on the developed materials was about 500 mAh g-1 at 200 mV polarization. The synthesized materials are stable and catalytically active.

Keywords: Reduced graphene oxide (RGO); Graphene Oxide; Electrode Materials; Fuel Cells; Oxygen Electrodes.

Introduction

The application of air or oxygen electrode in devices generating electrical energy is useful, it does not give rise to environmental problems and allows saving nonrenewable natural resources. Air and oxygen electrode is a three-phase electrode-electrolyte-gas system, where the generation of electric current is localized at the phase boundary. The current magnitude generated at such gas diffusion electrode depends on the triple contact zone of these three phases. In its turn, the electrode itself is composed of catalyst and carrier. The interaction between them determines the quantity of generated current, which depends on the catalyst used. It is known that nowadays the most effective catalyst for oxygen reduction is platinum, which is a very expensive material. A great number of works are dedicated to the investigation of other effective but less costly catalysts [1]. Another problem is catalytically active and stable carrier. In works the advantages of carbon nanotubes used as the carrier are shown [2-4]. At the present time, graphene begins to be used in lithium ion batteries and current sources, as a catalyst support for fuel cell electrodes [5-10].

At the moment, the following methods for the synthesis of graphene from carbon nanotubes are known: intercalation of alkaline earth elements and nitrogen; plasma etching; microwave unzipping; unzipping with catalytic metal nanoparticles; ultrasonic unzipping; opening-up by laser irradiation; electrical unzipping; hydrogenation at high-temperature; unzipping by means of a scanning tunnel microscope; electrochemical unrolling; redox chemical synthesis [11-29].

The chemical synthesis of graphene involves the step of obtaining graphene oxide (GO) and its subsequent reduction to give the so-called the reduced graphene oxide (RGO). Carbon nanotubes have a rigid structure of graphene layers, which leads to a decrease in binding energy between the carbon atoms in the graphene layer. Using a suitable oxidant, one can longitudinally "unzip" nanotubes to form GO nanoribbons and then obtain RGO by the action of a reductant. The synthesis, structure and chemical properties of GO and RGO were systematized and described in detail in reviews [28-31].

The purpose of the work is synthesis and study of the properties of graphene oxide and RGO, which are used as a catalyst for the oxygen electrodes of fuel cells.

Affiliation:
[1]*Vernadskii Institute of General & Inorganic Chemistry of Nat Acad Sci Ukraine, Prospekt Palladina 32-34, 03680 Kyiv 142, Ukraine*

[2]*Institute of Sorption and Problems of Endoecology of Nat Acad Sci Ukraine, general Naumov st. 13, 03164 Kiev, Ukraine*

***Corresponding author:**
Rusetskii IA, Vernadskii Institute of General & Inorganic Chemistry of Nat Acad Sci Ukraine, Prospekt Palladina 32-34, 03680 Kyiv 142, Ukraine, Tel: +380 44 4242280
E-mail: rusetskii@ionc.kiev.ua

Citation: Danilov MO, Rusetskii IA, Slobodyanyuk, IA Farbun, Kolbasov G Ya (2015) Synthesis and Electrocatalytic Properties of Materials Based On Graphene Structures. NMCT 104:1-5

Received: Oct 01, 2015
Accepted: Jan 25, 2016
Published: Feb 01, 2016

Experimental

We used purified reagents: H_2SO_4 (98%), HF (40%), HCl (35%), $KMnO_4$, $NaH_2PO_2 \cdot H_2O$, H_2PtCl_6, $Pb(CH_3COO)_2 \cdot 3H_2O$, KOH. For the preparation of solutions and washing we took bidistilled water. As a precursor we used multi-walled carbon nanotubes (MWCNT), obtained by the catalytic pyrolysis of acetylene on a catalyst.

The outer diameter of MWCNTs was about 10-30nm, with a bulk density of 25-35gdm^{-3}. The number of walls was 8-15. MWCNTs were purified of catalyst by means of hydrofluoric acid treatment. Platinum is deposited by electrochemical method from an aqueous solution containing 3%H_2PtCl_6 and 0.2mass% lead acetate(II) at a voltage of 1V for 2minutes, the current direction is changed through 30s.

Based on the standard redox potentials of carbon (Table 1) the required oxidant potential in acid medium should be more than +0.528V and oxidant potential in alkaline medium should be more than –0.603V [32]. However, if the process of breaking carbon bonds in nanotubes is due to kinetic constraints, then the use of thermodynamic redox scale for this process is not possible.

Accordingly, for the reduction of graphene oxide in alkaline medium reducing agents with potentials under –1.148V must be used. In an acidic environment, reducing agents with potentials under –0.320V must be used to reduce GO. As reducing agents in an alkaline medium we used solutions of sodium hypophosphite ($E^{\ominus}$ = –1.51V) [32-33].

One gram of MWNTs was dispersed in 300ml of concentrated sulfuric acid with stirring for one hour. Then 5g of $KMnO_4$ was added and stirred in an oil bath for one hour at a temperature not exceeding 17°C. Thereafter, the mixture was heated in an oil bath to 55°C for 30minutes. Then, the temperature was adjusted to 65°C, the mixture was allowed to stand for 20minutes and cooled to room temperature. To remove possible by-product (manganese dioxide), the resulting mixture was poured into 400ml of bidistilled water and ice, which contained 5ml of 30 mass% H_2O_2. This mixture filtered using fine - pored filter paper. The filter cake was transferred to a colloidal solution in bidistilled water. A sample of obtained graphene oxide was dried at 140°C for three hours and used for the studies. Another sample of oxidized product was reduced with an alkaline solution of sodium hypophosphite (pH=11). The resulting reduced graphene oxide was filtered using a dense, fine-pored filter paper and then separated from the filter and dried in an oven at 140°C for three hours. The samples of RGO obtained by synthesis were examined with the aid of a JEM-100 CXII electron microscope. The synthesized graphene samples were examined with an electron microscope JEM-100 CXII. The X-ray phase analysis was performed with the aid of a DRON-4 X-ray diffractometer with CuK_a radiation.

The porous structure of graphene materials was studied by low-temperature nitrogen adsorption. The nitrogen adsorption/desorption isotherms were recorded at -196°C using a gas surface analyzer NOVA 2200 (Quantachrome, USA). The parameters of the porous structure of the samples (the specific surface area, the volume of sorption pores, effective pore radius), and the volume distribution of the pore size were calculated using the program AsiQ version 3.0 for the calculations we used the BET method, the t-method, BJH and DFT. Before the measurements, the degassing of samples at 180°C was carried out under pressures of 1.10^{-4}Torr for 20hours.

The synthesized materials were used as the active layer of the oxygen electrode. The hydrophobic layer contained 0.07gcm^{-2} acetylene black with 25% polytetrafluoroethylene, and the active layer contained 0.02gcm^{-2} RGO with 5% polytetrafluoroethylene. The investigations were carried out on a fuel cell mockup, a zinc electrode being used as the anode. A mockup for the testing of gas-diffusion electrodes is described in Reference [34]. The electrolyte was a solution of 6M KOH. A silver-chloride electrode connected through a salt bridge was used as a reference electrode. The electrochemical characteristics were recorded under galvanostatic conditions. The study of the polarization curves was performed on a P-8S Elins (Russia) potentiostat on a standard three-electrode system. The oxygen source was a U-shaped electrolyzer with alkaline electrolyte. Oxygen was supplied to the gas electrodes under an excess pressure of 0.01MPa. Before measurements, the oxygen electrode was blown through with oxygen for an hour.

Results and Discussion

Figure 1 shows micrographs of GO obtained by oxidation of MWCNTs using potassium permanganate. **Figure 1**

Figure 2 shows a micrograph of RGO obtained by reduction with sodium hypophosphite the GO obtained by oxidation of MWCNTs using potassium permanganate. **Figure 2**

Figure 3 shows the X–ray diagrams of initial multiwalled carbon nanotubes (a), graphene oxide (b) and reduced graphene oxide (c). **Figure 3**

The XRD analysis showed the presence of two peaks, one of which corresponds to the reflection from the interplanar spacing between the graphene layers and is located at 2θ=25.6°, and the other near 2θ=21° corresponds to SiO_2 (substrate), the distance

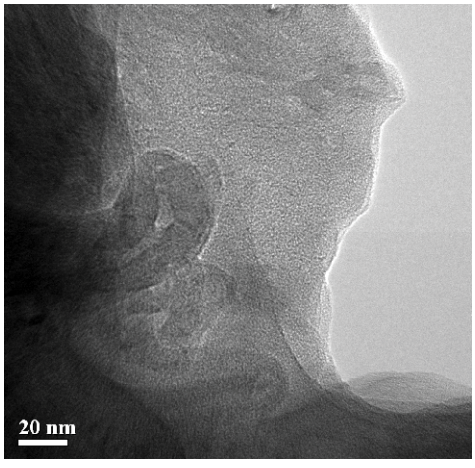

Figure 1: Micrographs of a sample of GO obtained from MWCNTs oxidized with $KMnO_4$.

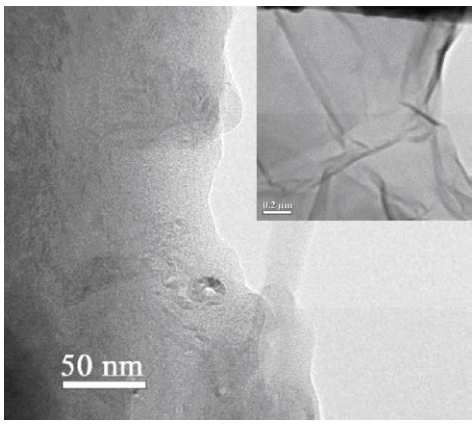

Figure 2: Micrograph of a sample of RGO obtained from MWCNTs oxidized with $KMnO_4$ and reduced with sodium hypophosphite.

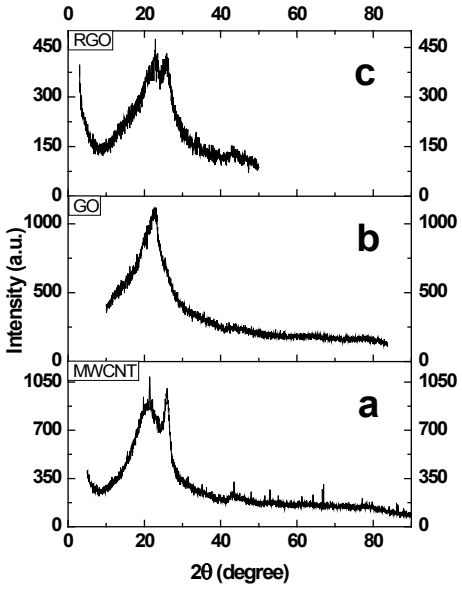

Figure 3: X-ray diagrams of samples of initial MWCNTs (a), graphene oxide (b) and reduced graphene oxide (c).

between the planes in RGO is found to be 3.43Å, which is larger than the distance between the planes in graphite (3.35Å). The initial carbon nanotubes and samples of synthesized RGO have similar reflections; in the case of RGO reflection at 2θ=25.6° becomes wider, the crystallinity of the RGO sample deteriorates, which indicates a decrease in the size of particles.

The nitrogen adsorption/desorption isotherms, measured for MWCNT samples, GO and RGO, differ greatly from each other not only in form but also in the volume of adsorbed nitrogen (Figure 4). **Figure 4**

For all samples, the initial part of the isotherm, which refers to the microporous region, is very small. For the sample of MWCNTs, presence on the isotherm of a hysteresis loop at medium and high pressure, as well as a sharp rise in the isotherm at the pressure P/Po>0.9 indicate that the structure of the sample is made up of meso and macropores. In the nitrogen adsorption/desorption isotherm for the sample of graphene oxide, an expansion of the hysteresis loop is observed, which indicates a decrease in the number of macropores and an increase in the proportion of mesopores in the total pore volume (type II of IUPAC classification with H3 hysteresis loop) [34,35]. For the sample of reduced graphene oxide, the main cause of hysteresis at low pressures (P/Po<0.4) is activated passage of molecules into wider cavities through existing constrictions [36].

The presence of macropores in the structure of the MWNT sample proves the difference in the values of the specific surface area of this sample, obtained by the BET method (Table 1) and the BJH method (149.2m^2g^{-1}). **Table 1**

Oxidation of MWCNTs to GO increases the specific surface area by a factor of 2, reduces the pore radius and increases the number of micropores. Since the nanopores region (0.5 to 50nm) accepted in the literature covers micro- and mesopores, all test samples are nanoporous materials with predominance of mesopores [37].

Figure 5 shows differential pore volume distribution curves, obtained from the desorption branch of nitrogen capillary condensation using the BJH method. **Figure 5**

It can be seen from Figure 5 that the most coarse - pored material is MWCNTs with an average pore size of ≈50nm. Oxidation of MWCNTs to GO leads to the appearance of a narrow peak (r=1.5-3nm), indicating a narrow pore volume distribution by size.

When analyzing the pore volume distribution by size by the DFT method, was found that in the sample of MWCNTs there are mesopores with ≈10-20nm size (Figure 5b). The oxidation of MWCNTs to GO leads to the appearance of mesopores with 1.0-1.5 and 2-3nm size.

Sample	$S_{sp.}$[1], m2 g-1	$V_{tot.}$[1], *cm3 g-1*	V_{meso}[2], *cm3 g-1*	V_{micro}[1,2], *cm3 g-1*	Micropore fraction, %	r_{mean}[1], nm	r_{des}[2], nm
MWCNT	126,3	2,77	2,76	0,01	0,36	43,8	16,2
GO	231,4	0,45	0,44	0,01	2,22	3,9	1,9
RGO	3,5	–	0,006	–	0	–	1,8

[1]BET method, [2]BJH method.

Table 1: Porosity characteristics of MWNT, RGO and GO samples.

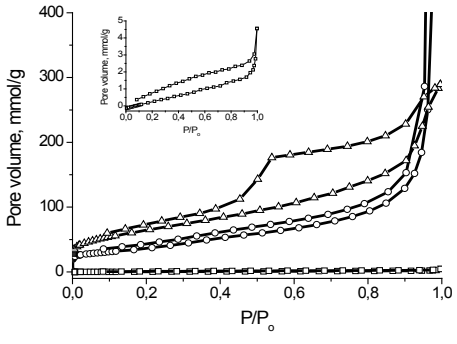

Figure 4: Nitrogen adsorption/desorption isotherms: MWCNTs (−○−), RGO (−□−) and GO (−Δ−).

The significant reduction of specific surface area is due to the fact that as graphene oxide reduced the hydrophilicity of its layers gradually decreases. The graphene sheets agglomerate and the precipitate cannot be redispersed even by ultrasonic (US) treatment [38]. To prevent agglomeration, molecules of surfactants, biomolecules, polymers, and large aromatic donor or acceptor molecules, which stabilize RGO by π-π interactions, are added to the reaction mixture [39-42].

Figure 6 shows the characteristics of oxygen electrodes based on GO (curve 2) and RGO (curve 3) and carbon nanotubes with 10 mass % platinum deposited on them (curve 4). **Figure 6**

As is seen from the current-voltage curves the electrodes based on RGO have better performance than the electrodes based on GO. The oxygen electrodes based on graphene oxide and reduced graphene oxide was stable for six month under galvanostatic conditions at a current density of 200mAcm^{-2}. For graphene oxide doped with sulfur and nitrogen, the value of specific capacity of 415mAhg^{-1} at 0.9V with respect to zinc electrode is given, which corresponds to approximately 300mV polarization. For reduced graphene oxide doped with nitrogen with deposited $LiMn_2O_4$ the value of specific capacity of 585mAhg^{-1} at 1.15V with respect to aluminum electrode is given, which corresponds to approximately 400mV polarization [43,44]. The specific capacity calculated for our electrodes at 200mV polarization is about 500mAhg^{-1}. Thus, the proposed simplified procedure for obtaining samples of oxidized graphene and reduced graphene oxide can produce materials for catalyst carriers which are not inferior to the existing analogues.

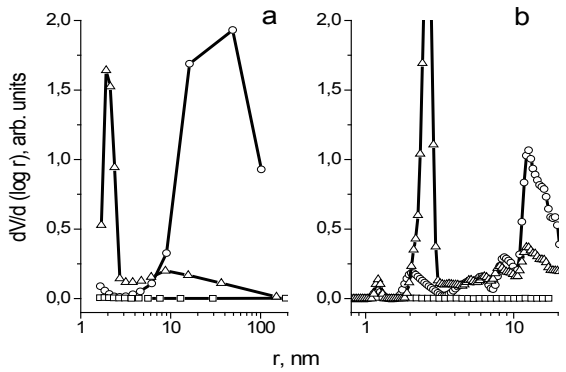

Figure 5: Differential pore volume distribution curves for samples of MWCNTs (−○−), RGO (−□−) and GO (−Δ−) obtained by the BJH (a) and DFT (b) methods.

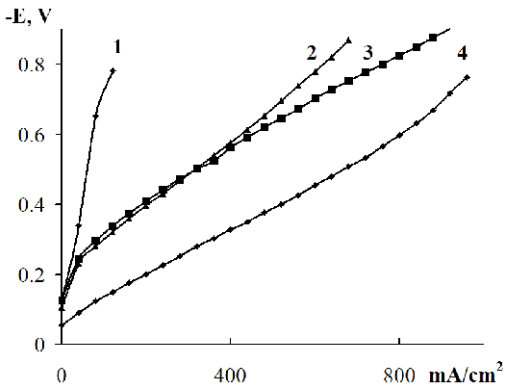

Figure 6: Load characteristics of oxygen electrodes with different active layer: initial MWCNTs (1); graphene oxide (2); reduced graphene oxide (3); MWCNTs with deposited 10 mass % Pt (4).

Conclusions

The synthesized graphene oxide and reduced graphene oxide promise much as catalyst carriers for the oxygen electrode of fuel cell, which can replace the commercial electrode materials containing platinum.

References

1. Bidault F, Brett DJL, Middleton PH, et al. Review of gas diffusion cathodes for alkaline fuel cells (2009) J Power Sourc 187: 39–48.
2. Soehn M, Lebert M, Wirth T, et al. Design of gas diffusion electrodes using nanocarbon (2008) Ibid 176: 494–498.
3. Hsieh CT, Lin JYi, Wei JL. Deposition and electrochemical activity of Pt-based bimetallic nanocatalysts on carbon nanotube electrodes (2009) Int J Hydrogen Energy 34: 685–693.
4. Wang X, Waje M, Yan Y. CNT-Based Electrodes with High Efficiency for PEMFCs (2005) Electrochem Solid-State Lett 8: A42–A44.
5. Wang G, Shen X, Yao J, et al. Graphene nanosheets for enhanced lithium storage in lithium ion batteries (2009) Carbon 8: 2049–2053.
6. Xin Y, Liu J, Jie X, et al. Preparation and electrochemical characterization of nitrogen doped graphene by microwave as supporting materials for fuel cell catalysts (2012) Electrochim Acta 60: 354–358.
7. Lin Z, Waller G, Liu Y, et al. Facile synthesis of nitrogen-doped graphene via pyrolysis of graphene oxide and urea and its electrocatalytic activity toward oxygen reduction reaction (2012) Adv Energy Mater 2: 884–888.
8. Qu L, Liu Y, Baek JB, et al. Nitrogen-doped graphene as efficient metal-free electrocatalyst for oxygen reduction in fuel cells (2010) ACS Nano 4: 1321-1326.
9. Lin Z, Song MK, Ding Y, et al. Facile preparation of nitrogen-doped graphene as a metal-free catalyst for oxygen reduction reaction (2012) Phys Chem Chem Phys 14: 3381-3387.
10. Shao Y, Zhang S, Wang C, et al. Highly durable graphene nanoplatelets supported Pt nanocatalysts for oxygen reduction (2010) J Power 195: 4600–4605.
11. Cano Márquez AG, Rodriguez Macias FJ, Campos Delgado J, et al. Ex-MWNTs: Graphene sheets and ribbons produced by lithium intercalation and exfoliation of carbon nanotubes (2009) Nano Lett 9: 1527–1533.
12. Kosynkin DV, Lu W, Sinitskii A, et al. Highly conductive graphene nanoribbons by longitudinal splitting of carbon nanotubes using potassium vapor (2011) ACS Nano 5: 968-974.
13. Morelos-Gómez A, Vega-Díaz SM, González VJ, et al. Clean nanotube unzipping by abrupt thermal expansion of molecular nitrogen: graphene nanoribbons with atomically smooth edges (2012) Ibid 6: 2261–2272.
14. Jiao L, Zhang L, Wang X, et al. Narrow graphene nanoribbons from carbon nanotubes (2009) Nature 458: 877-880.
15. Valentini L. Formation of unzipped carbon nanotubes by CF4 plasma treatment (2011) Diamond & Related Materials 20: 445–448.
16. Mohammadi S, Kolahdouz Z, Darbari S, et al. Graphene formation by unzipping carbon nanotubes using a sequential plasma assisted processing (2013) Carbo 52: 451–463.
17. Janowska I, Ersen O, Jacob T, et al. Catalytic unzipping of carbon nanotubes to few–layer graphene sheets under microwaves irradiation (2009) Appl Catal V 371: 22–30.
18. Vadahanambi S, Jung J–H, Kumar R. et al. An ionic liquid-assisted method for splitting carbon nanotubes to produce graphene nano–ribbons by microwave radiation (2013) Carbon 53: 391–398

19. Elías A.L, Botello-Méndez As.R, Meneses-Rodríguez D. et al. Longitudinal cutting of pure and doped carbon nanotubes to form graphitic nanoribbons using metal clusters as nanoscalpels (2009) Nano Lett 10: 366–372

20. Parashar UK1, Bhandari S, Srivastava RK, Jariwala D, Srivastava A. Single step synthesis of graphene nanoribbons by catalyst particle size dependent cutting of multiwalled carbon nanotubes (2011) Nanoscale 3: 3876-3882.

21. Jiao L1, Wang X, Diankov G, Wang H, Dai H. Facile synthesis of high-quality graphene nanoribbons (2010) Nat Nanotechnol 5: 321-325.

22. Xie L1, Wang H, Jin C, Wang X, Jiao L, et al. Graphene nanoribbons from unzipped carbon nanotubes: atomic structures, Raman spectroscopy, and electrical properties (2011) J Am Chem Soc 133: 10394-10397.

23. Kumar P1, Panchakarla LS, Rao CN. Laser-induced unzipping of carbon nanotubes to yield graphene nanoribbons (2011) Nanoscale 3: 2127-2129.

24. Kim K1, Sussman A, Zettl A. Graphene nanoribbons obtained by electrically unwrapping carbon nanotubes (2010) ACS Nano 4: 1362-1366.

25. Talyzin AV1, Luzan S, Anoshkin IV, Nasibulin AG, Jiang H, et al. Hydrogenation, purification, and unzipping of carbon nanotubes by reaction with molecular hydrogen: road to graphane nanoribbons (2011) ACS Nano 5: 5132-5140.

26. Paiva MC1, Xu W, Proença MF, Novais RM, Laegsgaard E, et al. Unzipping of functionalized multiwall carbon nanotubes induced by STM. (2010)Nano Lett 10: 1764-1768.

27. Shinde DB1, Debgupta J, Kushwaha A, Aslam M, Pillai VK. Electrochemical unzipping of multi-walled carbon nanotubes for facile synthesis of high-quality graphene nanoribbons (2011) J Am Chem Soc 133: 4168-4171.

28. Kosynkin DV1, Higginbotham AL, Sinitskii A, Lomeda JR, Dimiev A, et al. Longitudinal unzipping of carbon nanotubes to form graphene nanoribbons (2009) Nature 458: 872-876.

29. Zhang S., Zhu L., Song H. et al. How graphene is exfoliated from graphitic materials: synergistic effect of oxidation and intercalation processes in open, semi-closed, and closed carbon systems (2012) J. Mater. Chem 22: 22150–22154

30. Zhu Y1, Murali S, Cai W, Li X, Suk JW, et al. (2010) Graphene and graphene oxide: synthesis, properties, and applications. See comment in PubMed Commons below Adv Mater 22: 3906-3924.

31. Pei S, Cheng H.M. The reduction of graphene oxide (2012) Carbon 50: 3210–3228

32. Bratsch S.G. Standard electrode potentials and temperature coefficients in water at 298.15 (1989) J. Phys. Chem 18: 1–21

33. Danilov M.O, Kolbasov G.Ya, Rusetskii I.A. et al. Electrocatalytic properties of multiwalled carbon nanotubes-based nanocomposites for oxygen electrodes (2012) Russian J. Appl. Chem 85: 1536–1540

34. Gregg S.J, Sing K.S.W. Adsorption, surface area and porosity (1982) London: Academic Press 310

35. Sing K.S.W, Everett D.H, Haul R.A.W. et al. Reporting physisorption data for gas/solid systems with special reference to the determination of surface area and porosity (1985) Pure Appl. Chem 57: 603–619

36. Zhang P, Xu F, Navrotsky A. et al. Surface enthalpies of nanophase ZnO with different morphologies (2007) Chem 19: 5687-5693

37. Edelstein A.S., Cammarata K.C. Nanomaterials: synthesis, properties and applications (1998) Washington: CRC Press 616

38. Stankovich S, Dikin D.A, Piner R.D, et al. Synthesis of graphene-based nanosheets via chemical reduction of exfoliated graphite oxide (2007) Carbon 45: 1558-1565

39. Stankovich S1, Dikin DA, Dommett GH, Kohlhaas KM, Zimney EJ, et al. (2006) Graphene-based composite materials. See comment in PubMed Commons below Nature 442: 282-286.

40. Patil A.J, Vickery J.L, Scott Th. B Mann S. Aqueous stabilization and self-assembly of graphene sheets into layered bio-nanocomposites using DNA (2009) Adv. Mater 21: 3159-3164

41. Xu Y, Bai H, Lu G, et al. Flexible graphene films via the filtration of water-soluble noncovalent functionalized graphene sheets (2008) J. Am. Chem. Soc 130: 5856-5857

42. Liu H, Gao J, Xue M, et al. Processing of graphene for electrochemical application: noncovalently functionalize graphene sheets with water-soluble electroactive methylene green (2009) Langmuir 25: 12006-12010

43. Ganesan P, Ramakrishnan P, Prabu M, Shanmugam S. Nitrogen and Sulfur Co-doped Graphene Supported Cobalt Sulfide Nanoparticles as an Efficient Air Cathode for Zinc-air Battery (2015) Electrochim. Acta 183: 63-69

44. Liu Y, Li J, Li W, et al. Spinel LiMn2O4 nanoparticles dispersed on nitrogen-doped reduced graphene oxide nanosheets as an efficient electrocatalyst for aluminium-air battery (2015) International Journal of Hydrogen 40: 9225-9234